NASA Technical Memorandum 106327
AIAA–93–1953

Axisymmetric Single Shear Element Combustion Instability Experiment

Kevin J. Breisacher
Lewis Research Center
Cleveland, Ohio

Corrected Copy

Prepared for the
29th Joint Propulsion Conference and Exhibit
cosponsored by the AIAA, SAE, ASME, and ASEE
Monterey, California, June 28–30, 1993

National Aeronautics and
Space Administration

Axisymmetric Single Shear Element Combustion Instability Experiment

by

Kevin J. Breisacher
NASA Lewis Research Center

Abstract

The combustion stability characteristics of a combustor consisting of a single shear element and a cylindrical chamber utilizing LOX and gaseous hydrogen as propellants are presented. The combustor geometry and the resulting longitudinal mode instability are axisymmetric. Hydrogen injection temperature and pyrotechnic pulsing were used to determine stability boundaries. Mixture ratio, fuel annulus gap, and LOX post configuration were varied. Performance and stability data are presented for chamber pressures of 300 and 1000 psia.

Introduction

Currently, a rigorous calculation of the combustion stability of a large liquid rocket engine is not feasible. Computationally these calculations are infeasible due to the inherent three dimensionality of the most common instability mode shapes and the fact that flight engines typically contain several hundred injection elements. Parallel computing may offer some hope of resolving this computational dilemma. However, even if sufficient computational resources were brought to bear on the problem, the lack of validated models for atomization, droplet dynamics, and droplet combustion in a rocket combustor environment would still prevent a rigorous solution from being obtained. One of the problems of validating such models for combustion instability is that the majority of existing experimental data is for three dimensional, multi-element geometries. Even "2D combustors" are three dimensional from a modeling standpoint. The ability to do "numerical experiments" to develop and validate new models without gross simplifications of the actual phenomena is severely limited by the existing experimental database. Complex multi-element geometries also make it difficult to apply diagnostics to obtain data for model validation. Finally, the cost of obtaining data from multi-element hardware is prohibitive.

The goal of this experimental program was to obtain data from a simple system that could be driven unstable yet retain the essential physics of the instability phenomena in a two dimensional geometry. This data would provide a unique validation test case for combustion instability models. By maintaining a true two dimensional geometry, models can take advantage of the inherent computational efficiencies of two dimensional calculations without unrealistic physical assumptions. The simplest system, of

course, would contain a single element. SP-194[1], the historical monograph on combustion instability, does not include single element engines in its section on research hardware. There does not appear to be a great amount of documentation devoted to single element instability experiments in the open literature.[2,3] However, the incentives to perform single element stability tests in the past were not as great as they are today.

A single shear coaxial element and a long, narrow cylindrical chamber were selected for this test program. The element was not recessed to further simplify the atomization process. Instabilities were to be initiated using low temperature hydrogen injection and pyrotechnic pulsing. Hydrogen temperature ramping is a well established method of inducing instabilities. The fuel side of a coaxial injection element can be thought of as a high pass filter whose gain is increased as hydrogen temperature is decreased. As the fuel side response is increased, so is the chance of triggering an instability. The LOX post was designed to have a resonance corrresponding to the first longitudinal (1L) mode of the chamber. Although the first tangential is the most common mode of concern, the first longitudinal was selected to preserve the two dimensionality of the experiment. It is understood that at the most fundamental level LOX jet oscillations and jet surface wave phenomena may violate the two dimensionality of the experimental setup. However, at present, the necessity of including these phenomena in instabilty models is unclear.

Test Engine

The test engine consisted of a single, coaxial injection element and a heat sink chamber (Figures 1 and 2). The chamber was 2.055" in diameter and was 18.25" in length from the injector face to the nozzle throat. The chamber consisted of a short injector section, a long main chamber assembly made of Hastalloy, and the throat section. A schematic representation of the engine is provided in Figure 3. The throat diameter was .592" and .296" for 300 and 1000 psia respectively. The chamber was instrumented with an array of seven high frequency, piezoelectric, pressure transducers (Figure 4.). The transducers were flush-mount, helium cooled, and had flat response to 20KHz. Three transducers were located circumferentially around the chamber 1.75" downstream of the injector face. The remaining four transducers were placed axially along the chamber. In addition to the high frequency pressure transducers, an array of nine static pressure transducers were placed axially along the chamber (Figure 4.). These transducers were of the strain gauge bridge type and were accurate to 1/2%.

The injection element consisted of a two piece LOX post assembly (Figure 2.) and a faceplate with an opening for the fuel annulus. The injection element was designed to be modular. Fuel annulus diameter (D_f) could be varied by changing the faceplate. LOX post orifice location and injection tip diameter could be varied by

interchanging pieces of the two piece LOX post assembly. Three LOX post configurations were selected for testing (Figure 5.). All three configurations are 9.24" in length and are fed by a 1" diameter dome. This length was chosen so that the resonance of the LOX post would match the resonance of the chamber (approximately 1800 Hz).
LOX post configuration 1 in Figure 5 has a simple .9375" diameter tube with no orifice and was selected for its low LOX side pressure drop. Configuration 2 has a .0625" diameter orifice at the top of the tube. Configuration 2 represents the preferred configuration of engine manufacturers. Configuration 3 which has a .0625" diameter orifice at the bottom of the tube is similar to a design used in the Lewis LOX/H_2 instability test programs of the 1960's.

Test Facility and Operating Procedure

The tests were conducted at the Lewis Research Center Rocket Engine Test Facility. This is a 50,000 lbf sea-level rocket test stand equipped with an exhaust-gas muffler and scrubber. A pressurized propellant system was utilized to deliver the propellants to the engine from the storage tanks. The engine was mounted on the thrust stand to fire vertically into the scrubber where the exhaust gases were sprayed with water for cooling and sound suppresion. The oxygen propellant line was immersed in a liquid nitrogen bath. In addition, a LOX pre-chill of the engine hardware was required before ignition to ensure that liquid oxygen was flowing to the engine. Obtaining low temperature hydrogen at the engine was also critical in the performance of this test program. Due to the relatively small size of the hardware in relation to the facility, this was sometimes difficult. A plastic type foam was used to insulate the hydrogen line. For the tests with the lowest hydrogen injection temperatures, a "pre-stage" condition (low Pc) was maintained for several seconds to chill the hardware in order to obtain low temperature hydrogen at the engine. Liquid helium was also utilized to chill the hardware in an unsuccessful attempt to obtain even lower hydrogen temperatures. Ignition was obtained with a GH2/GOX torch igniter placed 3.31" downstream of the faceplate on the side of the engine.

During 22 tests the engine was pulsed (bombed) using electrically detonated RDX pellets. Although several tests were conducted using 10 grain pellets, 2.5 and 5 grain pellets were adequate to disturb the engine. The bomb port was located 3.25 inches downstream of the faceplate and was directed radially into the chamber. It was necessary to cover the RDX pellets with a thin layer of putty to protect them from pre-detonation due to the LOX pre-chill.

Results

Tests were conducted with LOX post configurations 1,2, and 3 at 300 psi and configurations 1 and 3 at 1000 psi. Fuel to oxidizer velocity ratio and fuel side pressure drop were varied by changing fuel annulus gap. Tests were conducted with hydrogen at ambient temperatures and at the lowest hydrogen temperature obtainable in the facility. Typically, mixture ratio was varied from 2.0 to 6.0 for each configuration tested.

C^* efficiency was calculated by determining the expermintal C^* from the following equation:

$$C^*_{exp} = \frac{P_c A_t}{W_p}$$

where

P_c - is the chamber pressure
A_t - is the throat area
W_p - is the propellant flowrate

(The chamber pressure used in this equation is the static pressure measurement nearest to the beginning of the contraction section.)

and dividing by the theoretical C^* determined for the operating conditions of the test. An array of nine pressure tranducers were used to obtain an axial static pressure profile along the engine. Before each day's testing, a plate was placed over the nozzle of the engine and the chamber was pressurized. Readings were taken with the static pressure transducer array at five pressurization levels that bracketed the target chamber pressure for the tests. A calibration curve was then developed using these in place readings. Figure 15. displays three axial pressure profiles for typical tests. Even when using the in place calibrations, the scatter is significant. The phenomena that is to be measured and the accuracy of the instrumentation are of the same order. However, it does appear that a zone of recirculation or energy release is detectable near the injector face.

The operating conditions and stability for selected tests are displayed in Tables I-IV. In these tables, operating conditions such as propellant flowrates and pressure drops, chamber pressure, and hydrogen injection temperature are presented. Performance is characterized by the C^* efficiency. An injection velocity ratio and a density weighted velocity ratio are provided to indicate the operating regime of the injection element. The geometry tested in a particular run is indicated by a LOX post configuration number (corresponding to Figure 5) and a fuel

annulus diameter (D_f). Bomb tests are indicated by a small 'b' next to the test number. A stability classification, an estimate of the amplitude and the frequency of any oscillation are also provided in the tables. Classically, an engine is declared unstable if an organized oscillation exceeds ten percent of chamber pressure. Above ten percent of chamber pressure the possibility of hardware damage becomes a real concern. In some research programs, an instability was said to have occurred if the amplitude of an organized oscillation exceeded the noise level of the combustor. For purposes of this paper, the stability of the engine is categorized as follows based on oscillation amplitude:

0 - 5% Pc stable
5 - 10% Pc marginally stable
> 10% Pc unstable.

The amplitude and frequency of the oscillations were obtained from expanded digitized traces of the high frequency pressure measurements.

The 300 psi chamber pressure data for configurations 2 and 3 are presented in Table I. The ambient temperature hydrogen tests with all the configurations tested were always stable. In Table I, ambient temperature hydrogen tests for configuration 2 (orifice at the top of the LOX post) are presented. For two of the tests, no organized oscillation was detectable. The remaining tests had oscillations that were 2-3 percent of chamber pressure. The fuel and LOX side pressure drops as a percentage of chamber pressure for these tests were very high. These high pressure drops for ambient temperature testing resulted from the fact that the same injection element hardware was to be used for low hydrogen temperature and 1000 psi chamber pressure tests.

The most interesting stability behavior of this test program was encountered with configuration 3 (orifice at the bottom of the LOX post) and a fuel annulus diameter of .235". With this configuration, instabilities with amplitudes greater than 10% of chamber pressure were obtained. All of the instabilities encountered with this configuration were spontaneously unstable. The oscillations are present from the beginning of mainstage and persist throughout the run with little frequency shift. This can clearly be seen in Figure 6 which displays the frequency content and relative amplitude (pressure) of the oscillation as the test progresses (time axis). The frequency content of the oscillations integrated over the duration of the test is provided in Figure 7. Figures 6 and 7 were obtained by applying Fourier Transforms to the digital samplings taken from the analog recordings of the high frequency pressure measurements. From Figure 7, the frequency and bandwidth of the oscillations are evident. The second harmonic is clearly present (Figures 6 and 7) and a trace of the third harmonic appears to be present also. To ensure that the two dimensionality of the oscillations was not being corrupted, Tests 286 and 292 were digitized at a sufficiently high rate to resolve

the first tangential mode for this combustor (17,100 Hz). There was no indication that a tangential mode of oscillation was occurring.
The waveforms produced by the unstable test cases are fairly complex. For test 286, very pronounced beating occurred (Figure 8). A comparison of Figure 8 and 9 suggests the beating is occurring between oscillations at approximately 1780 Hz and 1858 Hz. These modes probably correspond to the natural modes of the chamber and the LOX post. A higher beat frequency also appears to be occurring in Figure 8. and is produced by the first and second harmonics of the chamber oscillation. The oscillations appear to be limit cycle oscillations and do not appear to be very steep fronted. A number of the tests with this configuration had significant oscillation amplitudes but were not classically unstable. Figure 10. shows a plot of oscillation amplitude versus mixture ratio for configuration 3 with a fuel annulus diameter of .235". Injector pressure drop or hydrogen injection temperature effects are not shown on the plot, resulting in some of the scatter. However, the appearance of distinct operation regimes is clear. In particular, a tuning region between a mixture ratio of approximately 5 to 6 exists in which classic instabilities occur.

Retaining the same LOX post configuration but decreasing the fuel annulus diameter to .210" and .205" resulted in generally stable operation (Table I). Although an oscillation is present, its amplitude is between 3 and 5 percent of chamber pressure.

Configurations 2 and 3, both with orifices, had very high pressure drops. Eliminating the orifice, and utilizing a straight tube post (configuration 1) lowers the LOX side pressure drop. The results for configuration 1 are presented in Table II. The tests are generally stable. While the LOX side pressure drop is down, the fuel side pressure drops as a percentage of chamber pressure for the configurations in Table II are relatively high (greater than fifteen percent). The only test with an oscillation approaching significant amplitude (test 266), also has the minimum fuel side pressure drop. It would have been interesting to test this configuration with a larger fuel annulus gap.

By changing the throat diameter from .592" to .296", tests were run at a nominal chamber pressure of a 1000 psi with the same injection element hardware and propellant flowrates that were used at 300 psi. A chamber pressure of 1000 psi was selected because it is above the critical pressure of pure liquid oxygen. Test results for a chamber pressure of a 1000 psi are presented in Tables III and IV. When configuration 3 was run at 1000 psi the tests were very stable. In the majority of tests no organized oscillation is even detectable. It is interesting to note that when configuration 3 was tested at 1000 psi with a fuel annulus diameter of .235", the tests were stable. The same configuration was unstable at 300 psi. It is stable at 1000 psi even though the LOX and fuel side pressure drops as a percentage of chamber pressure are much lower than they were at 300 psi. Figure 11 displays the frequency content and amplitude relative to the

combustion noise level of an oscillation occurring during Test 369. Figure 12 provides the frequency and bandwidth of this oscillation integrated over the test duration. Figures 11 and 12 indicate that for configuration 1, while stable (Table III), an organized oscillation above the noise level of the combustor is clearly present. No harmonics of this oscillation are present. A comparison of Figures 11 and 12 with Figures 6 and 7, show that the oscillation occurring with configuration 1 at 1000 psi is of a narrower bandwidth. Plotting the variation of the oscillation amplitude with mixture ratio for this configuration there is significant scatter (Figure 13.). The scatter is not suprising since this oscillation is somewhat marginal to begin with. However, the trend is very similar to that of Figure 10. with a tuning region between a mixture ratio of 5 to 6.5 and falloff at higher and lower mixture ratios.

Bomb tests were performed during the test program (10 bomb tests are included in the tables). The bomb was triggered one half to one second before the end of a two second duration test. This timing provided ample time for a disturbance to organize and also permitted useful data to be taken before the bomb was triggered. Bomb overpressures ranged from 30 to 120 percent of chamber pressure. None of the bomb tests initiated an instability or altered the strength of an existing oscillation. The decay from a typical bomb pulse is shown in Figure 14.

Computational Models

A computational model of the test engine was made by modifying the KIVA II computer code.[4] The LOX tube flow was modeled using the one-dimensional "water hammer" equations. The LOX tube model provided the spray velocity and mass flowrate boundary conditions. The fuel side was modeled using a lumped parameter approach with the property variations during hydrogen temperature ramping being taken into account. The fuel side model provided a velocity boundary condition for KIVA II. A constant mass flowrate was imposed upstream of the LOX and fuel sides of the injection element. No attempt was made to resolve the atomization process computationally. A "blob" injection model with a dropsize correlation based on the work of Wu and Faeth[5] and a stochastic breakup model was employed. Results from the model for a stable, ambient temperature test and an unstable low temperature test are presented in Figure 16. The simulation of the high temperature test case exhibits small amplitude pressure oscillations whose frequency content is dominated by the first longitudinal oscillation. The low temperature simulation produces first longitudinal oscillations of an amplitude similar to those obtained experimentally for Test 286. It also appears as if beating is beginning to occur between the first and second harmonics (between 4.5 and 5.5 milliseconds in Figure 16). While the preliminary results look encouraging, the simulation should be carried out for longer than a few milliseconds. The initial goal is to reproduce the stabili-

ty (and corresponding performance) map shown in Figure 10. with a single dropsize correlation.

Summary

An axisymmetric LOX/GH_2 research engine with a single injection element was sucessfully test fired over a range of operating conditions. Stable and unstable combustion were observed when fuel annulus gap, LOX post design, mixture ratio, and chamber pressure were varied. Pulsing the engine with pyrotechnics did not induce instabilities. While no instabilities were triggered at a chamber pressure of a 1000 psi, interesting similarities with the unstable operating regimes encountered at 300 psi were noted.

Concluding Remarks

The data obtained in this test program provide a unique set of test cases for the validation of combustion instability codes, particularly CFD based models. Ultimately, it is hoped that validated instability codes could be used to design and predict the stability characteristics of future single element tests, a step on the path to reliable stability design codes for large liquid rocket engines.

References

1. Harrje, D. T. and Reardon, F. H., "Liquid Propellant Rocket Combustion Instability", NASA SP-194, 1972.

2. Harrje, D. T.,Reardon, F. H., and Crocco, L., "Combustion Instability in Liquid Propellant Rocket Motors", Princeton Univ. Aero. Eng. Rept. No. 216, Nov 1960.

3. Auble, C. M., "A Study of Injection Processes for Liquid Oxygen and Gaseous Hydrogen in a 200-Pound-Thrust Rocket Engine",NASA RM E56125a, Jan. 1957.

4. Amsden, A. A., O'Rourke, P. J., and Butler, T. D., "KIVA II: A Computer Program for Chemically Reactive Flows with Sprays", LA-11560-MS, May 1989.

5. Wu, P. K., Hsiang, L. P., and Faeth, G. M., "Aerodynamic Effects on Primary and Secondary Spray Breakup", First International Symposium on Liquid Rocket Combustion Instability, Pennsylvania State University, University Park, Pa.,Jan. 1993.

TABLE I.—TEST RESULTS FOR CONFIGURATIONS 2 AND 3 AT 300 psi

Test	Minimum H_2 injection temperature at ramp end, R	Static pressure at the injector, psia	Hydrogen weight flow, lbs/sec	Oxygen weight flow, lbs/sec	Mixture Ratio, O/F	H_2 ΔP	LOX ΔP	Characteristic exhaust velocity efficiency	Velocity injection ratio, V_g/V_l	$\rho V_g/\rho V_l$	Configuration, D_f (in.)	Stability classification	pk-pk Amplitude, %	Frequency, Hz
45	492	336	.079	.31	3.92	735	455	93.6	47	85	2 , .210	S	-	-
54	497	311	.0639	.30	4.69	504	416	96.1	48	67	"	S	2.5-3.0	1755
57	495	305	.059	.305	5.17	470	422	96.1	48	62	"	S	2.5-3.0	1663
58	496	306	.056	.309	5.51	424	424	95.4	47	60	"	S	-	-
90	497	303	.065	.30	4.96	464	414	94.9	48	68	"	S	2.5-3.0	1777
91	498	301	.056	.304	5.42	430	443	94.7	48	59	"	S	2.5-3.0	1738
93	498	303	.059	.31	5.25	448	436	93.3	47	64	"	S	2.0-2.5	1650
155	86	323	.088	.283	3.22	111	584	98.7	3.8	136	3 , .205	S	3.5	1755
159 b	85	322	.081	.274	3.38	95	589	100.5	3.6	121	"	S	3.0	2068
161	105	307	.060	.335	5.58	72	755	91.0	3.2	110	"	S	4.0	1630
163	108	302	.056	.315	5.63	75	787	94.5	3.4	97	"	S	2.5	2780
206	72	272	.081	.251	3.1	73	404	91.3	3.3	111	"	S	3.0	1743
208	92	252	.052	.282	5.42	54	552	87.5	3.4	80	"	S	3.0-4.5	1755
210	89	260	.053	.288	5.43	53	534	89.1	3.1	84	"	S	3.0	1759
212	89	272	.053	.314	5.92	48	621	87.1	2.86	91	"	S	3.0	1752
214	92	257	.054	.29	5.4	52	533	87.1	3.36	85	"	S	3.5-4.0	1807
216 b	91	261	.054	.33	6.16	54	669	85.6	2.9	97	"	S	3.0	1776
221	68	283	.085	.24	2.82	68	391	93.8	2.49	103	3 , .210	MS	5.0	1770
223	67	276	.085	.262	3.08	58	405	89.3	2.22	113	"	S	4.5-5.0	1777
225 b	68	278	.086	.26	3.02	53	420	87.7	2.42	114	"	S	3.5	1753
234	75	295	.058	.32	5.51	40	625	90.6	1.7	94	"	S	4.0	1754
276	71	294	.097	.243	2.51	38	384	95.8	2.28	86	3 , .235	S	2.5-3.0	1751
282 b	67	288	.096	.269	2.80	33	451	89.3	1.59	94	"	MS	6.0-7.0	1745
286 b	72	283	.061	.316	5.18	26	626	85.9	1.23	70	"	U	17.0	1782
288	71	292	.064	.328	5.13	22	644	85.7	1.13	77	"	MS	8.0	1860
292	75	301	.058	.345	5.94	25	715	87.4	1.10	73	"	U	13.0	1786
318	75	264	.081	.252	3.11	37	400	88.8	2.55	75	"	MS	6.5-7.0	1851
320	70	280	.080	.277	3.46	26	458	87.4	1.7	80	"	MS	7.0-7.5	1742
324	79	268	.062	.352	5.67	23	758	76.5	1.54	80	"	U	11.5	1822
326	78	289	.063	.361	5.73	24	791	79.3	1.34	83	"	U	10.5	1843
328	77	283	.057	.362	6.35	22	785	80.1	1.21	75	"	MS	5.0-5.5	1805
330	75	278	.056	.372	6.64	22	824	78.9	1.10	76	"	MS	9.0-9.5	1803
332 b	74	286	.057	.369	6.47	22	814	81.2	1.05	76	"	MS	7.0-7.5	1798

Note: A "b" next to a test number indicates a bomb test. A dash indicates that no discernible oscillation was present.

TABLE II.—TEST RESULTS FOR CONFIGURATION 1 AT 300 psi

Test	Minimum H_2 injection temperature at ramp end, R	Static pressure at the injector, psia	Hydrogen weight flow, lbs/sec	Oxygen weight flow, lbs/sec	Mixture Ratio, O/F	H_2 ΔP	O_2 ΔP	Characteristic exhaust velocity efficiency	Velocity injection ratio, Vg/Vl	ρVg/ρVl	Configuration, D_f (in.)	Stability classification	pk-pk Amplitude, %	Frequency, Hz
98	477	310	.083	.28	3.37	654	205	94.4	87	81	1, .210	S	1.5	3277
101	477	302	.087	.263	3.02	731	191	94.5	99	79	"	S	2.0-3.0	1940,3033
241	74	299	.057	.315	5.52	110	272	93.5	5.55	62	"	S	2.0	1777
245	72	314	.066	.29	4.39	107	229	99.7	5.89	66	"	S	1.5	1763
249	68	326	.123	.23	1.87	181	151	99.9	12.9	98	"	S	2.0	1979
258	70	302	.098	.242	2.46	82	146	99.8	6.24	51	1, .235	S	1.5	1777
262	71	305	.095	.268	2.82	73	179	97.8	5.7	55	"	S	1.5	1972
264 b	69	320	.092	.271	2.94	63	195	97.2	4.34	54	"	S	1.5	1972
266	74	287	.062	.304	4.90	46	231	89.8	4.16	41	"	S	4.0	1980
268 b	79	290	.061	.288	4.72	56	235	93.5	5.01	38	"	S	2.0	1979
298	85	299	.064	.378	5.91	62	383	80.0	4.48	52	"	S	-	
310	71	321	.079	.317	4.01	58	267	89.1	3.66	54	"	S	-	

TABLE III.—TEST RESULTS FOR CONFIGURATION 3 AT 1000 psi

Test	Minimum H_2 injection temperature at ramp end, R	Static pressure at the injector, psia	Hydrogen weight flow, lbs/sec	Oxygen weight flow, lbs/sec	Mixture Ratio, O/F	H_2 ΔP	O_2 ΔP	Characteristic exhaust velocity efficiency	Velocity injection ratio, Vg/Vl	ρVg/ρVl	Configuration, D_f (in.)	Stability classification	pk-pk Amplitude, %	Frequency, Hz
354	104	1053	.069	.244	3.54	16.5	345	93.9	.932	61	3 , .235	S	1.0-1.5	1892
356	117	1034	.049	.259	5.29	13.6	393	95.6	.759	45	"	S	1.5	1888
362	139	992	.042	.281	6.69	13.2	449	93.1	.79	42	"	S	1.0	1889
393	100	933	.055	.210	3.82	21	314	96.8	1.24	58	3 , .210	S	-	
397	103	1032	.045	.274	6.08	17.0	510	94.7	.75	62	"	S	-	
399	103	1044	.047	.279	5.94	11.8	493	94.1	.55	47	3 , .235	S	-	
401	87	1078	.069	.258	3.74	14.6	432	91.2	.67	63	"	S	1.0	1908
403	85	1057	.075	.244	3.25	16.2	385	92.1	.749	65	"	S	-	
411 b	97	1042	.053	.246	4.64	14.0	401	97.4	.64	47	"	S	2.0	1931
415	89	1102	.072	.241	3.35	17.0	380	99.9	.75	62	"	S	1.0	1789
426	95	964	.078	.192	2.46	27	213	100.2	1.72	75	3 , .210	S	-	

TABLE IV.—TEST RESULTS FOR CONFIGURATION 1 AT 1000 psi

Test	Minimum H_2 injection temperature at ramp end, R	Static pressure at the injector, psia	Hydrogen weight flow, lbs/sec	Oxygen weight flow, lbs/sec	Mixture ratio, O/F	H_2 ΔP	O_2 ΔP	Characteristic exhaust velocity efficiency	Velocity injection ratio, Vg/Vl	ρVg/ρVl	Configuration, D_f (in.)	Stability classification	pk-pk Amplitude, %	Frequency, Hz
337	95	1058	.055	.296	5.38	23	224	86.0	1.59	35	1 , .235	S	3.0-3.5	1879
369	107	1016	.047	.282	6.0	18.7	205	90.6	1.78	28	"	S	4.0	1821
373	101	954	.048	.322	6.70	17.7	244	77.4	1.53	33	"	S	3.0	1820
375	94	1001	.044	.304	6.91	16.5	215	87.4	1.27	28	"	S	3.0	1856
377	97	924	.033	.338	10.2	13.9	267	84.7	.96	23	"	S	1.5	1838
379	89	958	.039	.324	8.31	15.7	247	84.6	.99	27	"	S	1.0	1847
382	111	962	.053	.263	4.97	21	173	86.2	2.39	30	"	S	1.5	1883
384	105	997	.052	.281	5.40	19.7	190	85.9	1.95	31	"	S	1.0	1856
388	105	978	.051	.283	5.55	22	200	84.9	1.93	31	"	S	3.0	1865
405	88	1110	.063	.318	5.05	23	241	84.0	1.48	43	"	S	1.0	1878
409 b	89	1135	.058	.309	5.33	22	233	89.0	1.41	38	"	S	1.0	1870
420	93	921	.095	.183	1.93	24	220	94.8	4.75	37	"	S	-	

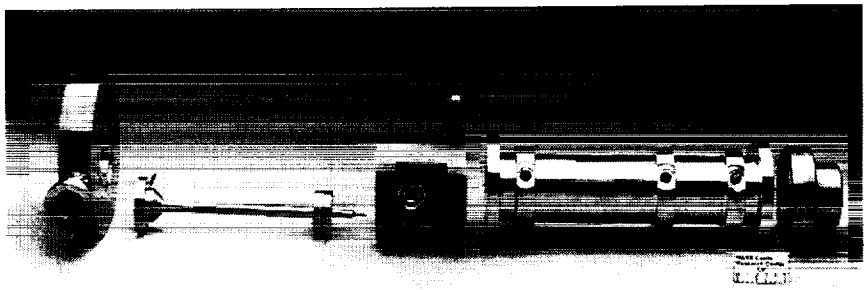

C-92 03422

Figure 1.—Single element test engine hardware.

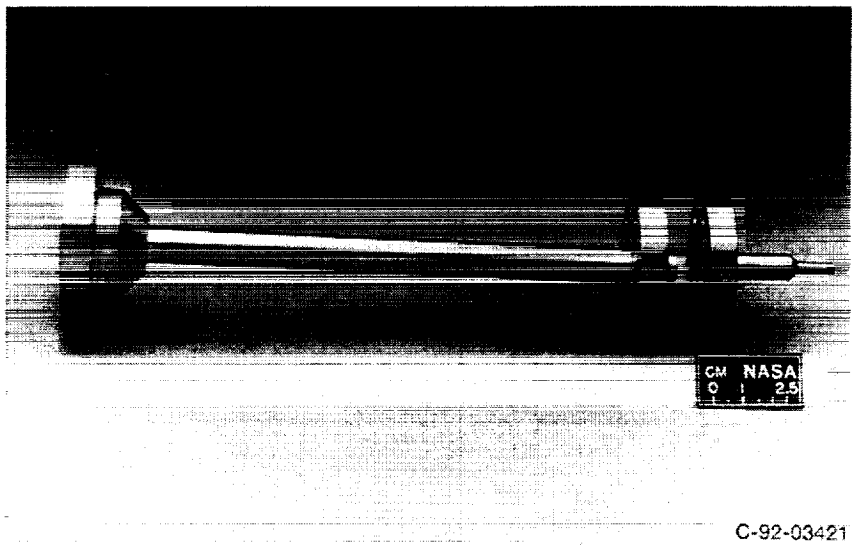

Figure 2.—LOX post assembly.

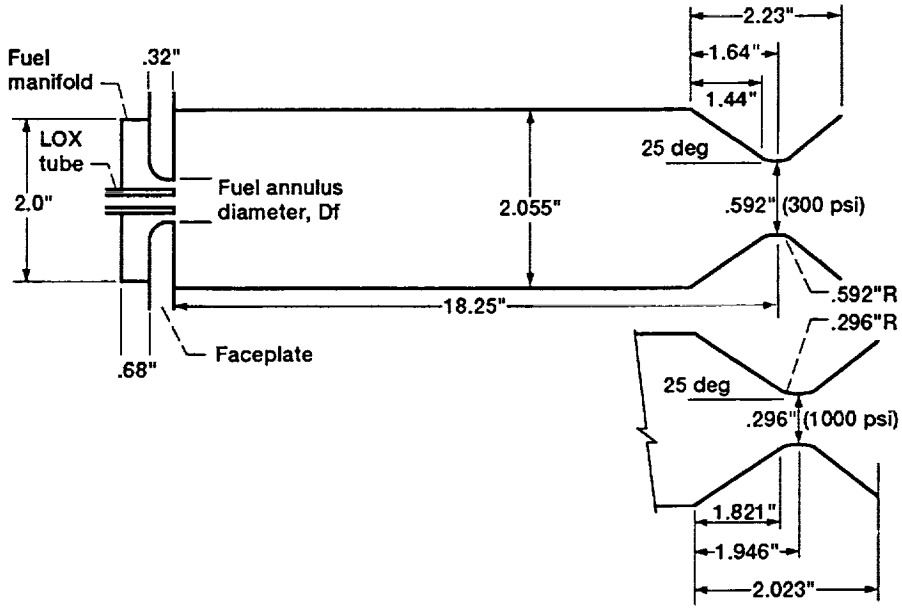

Figure 3.—Schematic representation of combustion chamber hardware.

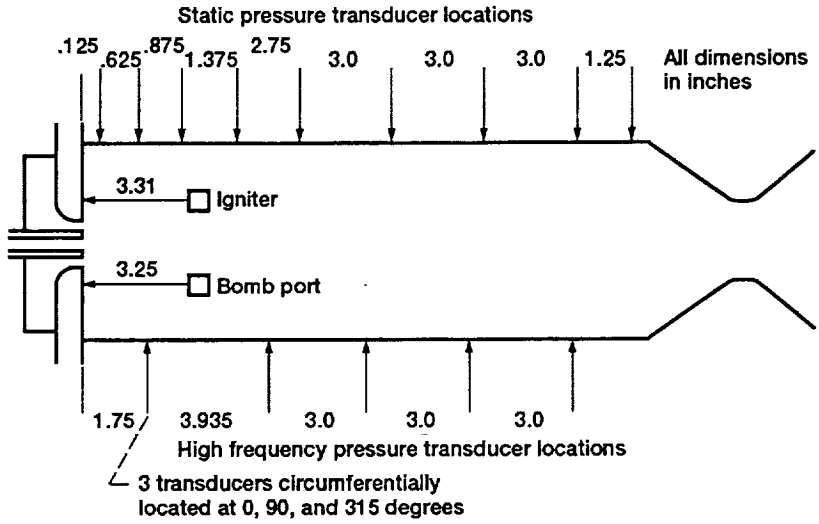

Figure 4.—Pressure transducer locations.

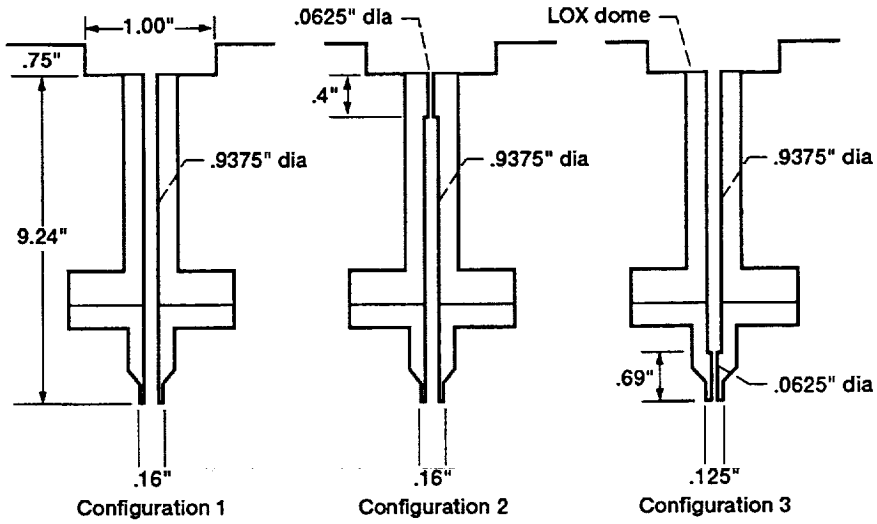

Figure 5.—Schematics of LOX post configurations.

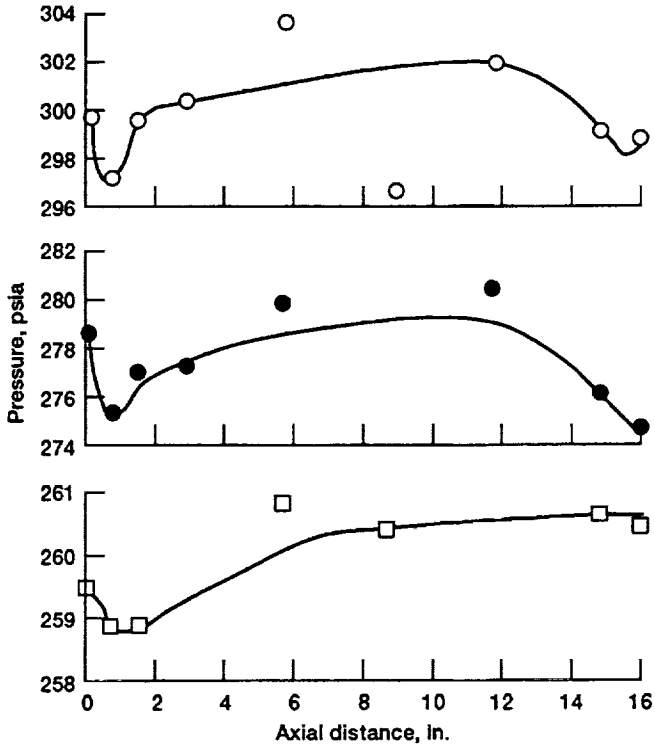

Figure 6.—Axial static pressure distribution.

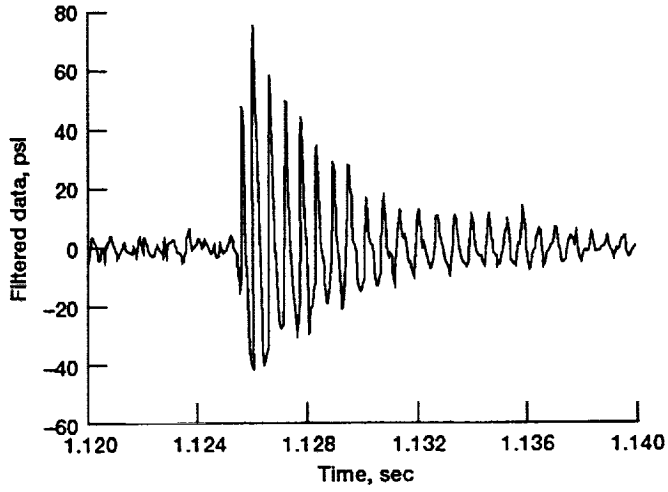

Figure 7.—Pressure history after 2.5 grain pulse (test 216).

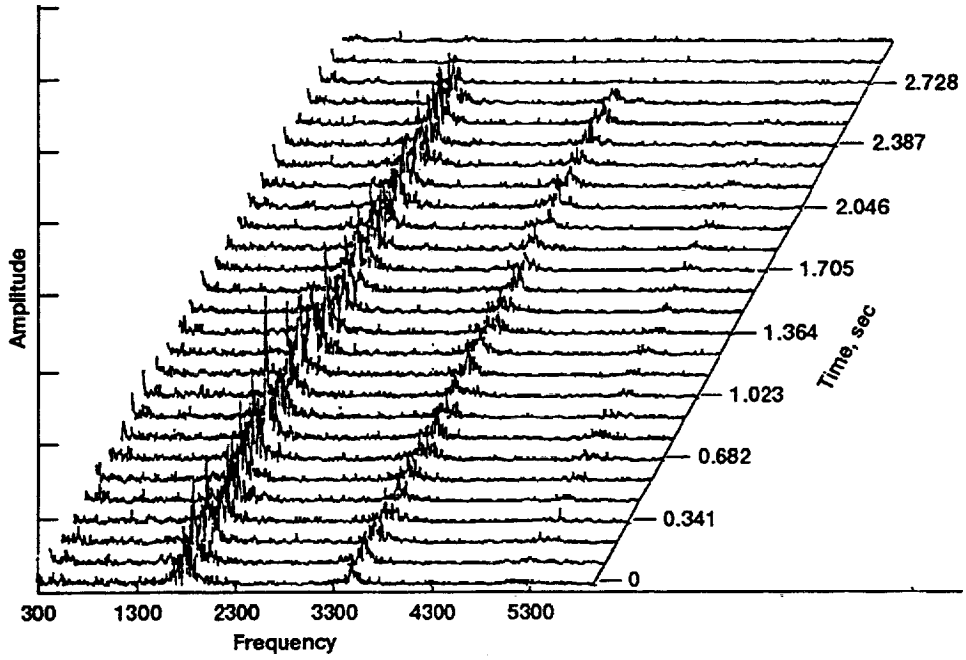

Figure 8.—Cascade plot of pressure for unstable test 292.

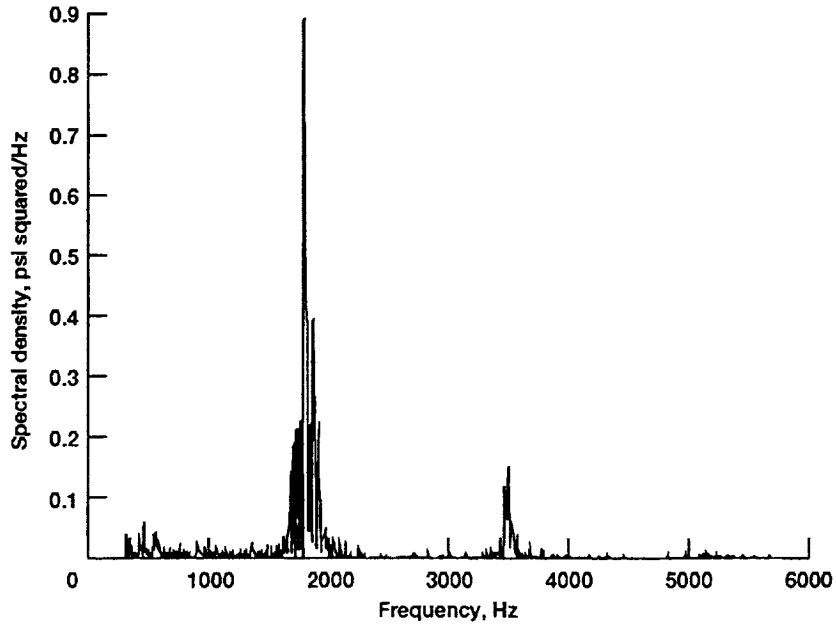

Figure 9.—Power spectral density plot for unstable test 292.

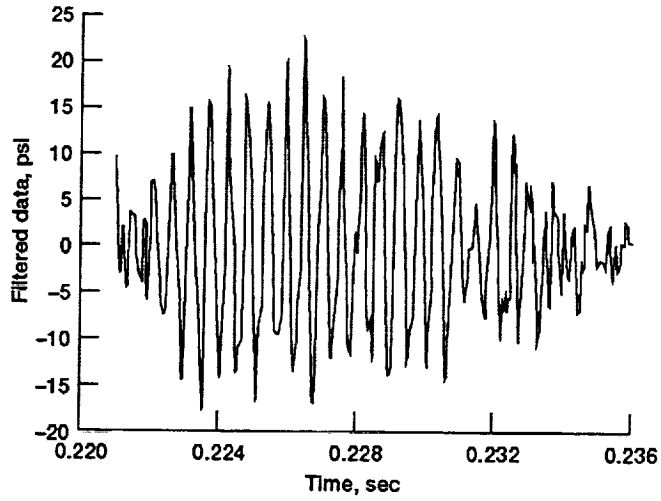

Figure 10.—Expanded digitized pressure trace for unstable test 286.

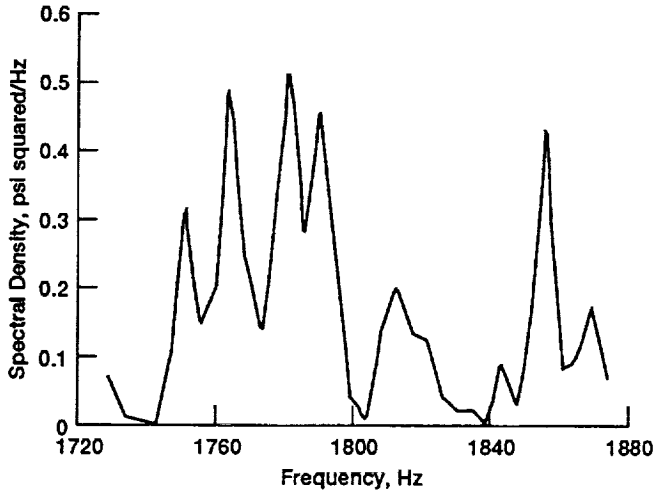

Figure 11.—Power spectral density plot for unstable test 286.

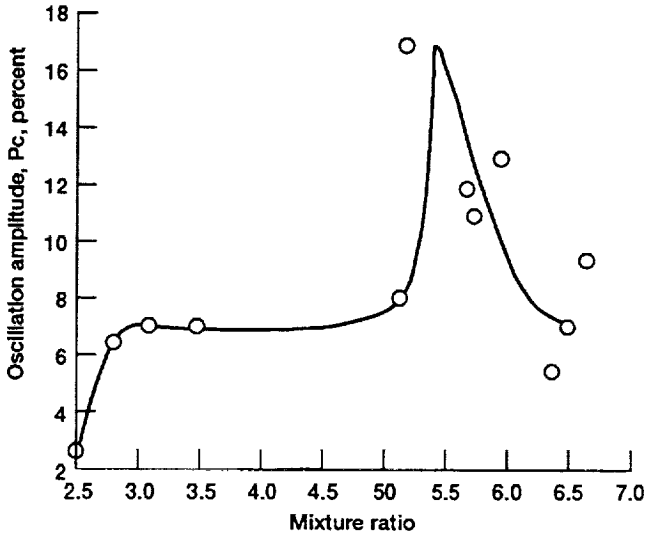

Figure 12.—Variation of oscillation amplitude with mixture ratio (configuration 3, Df - .235").

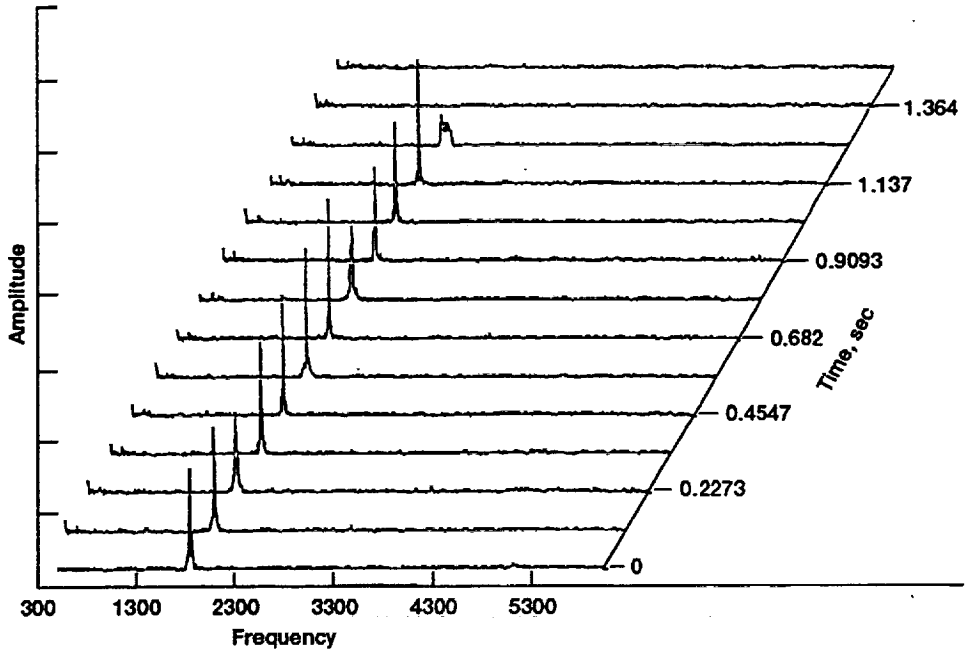

Figure 13.—Cascade plot of pressure for test 369.

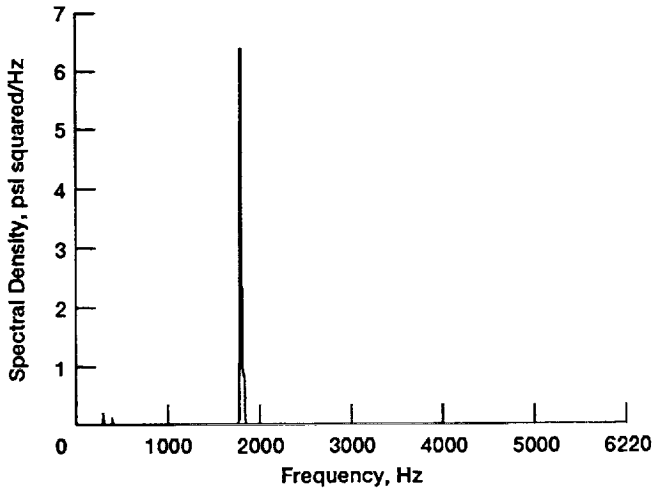

Figure 14.—Power spectral density plot for test 369.

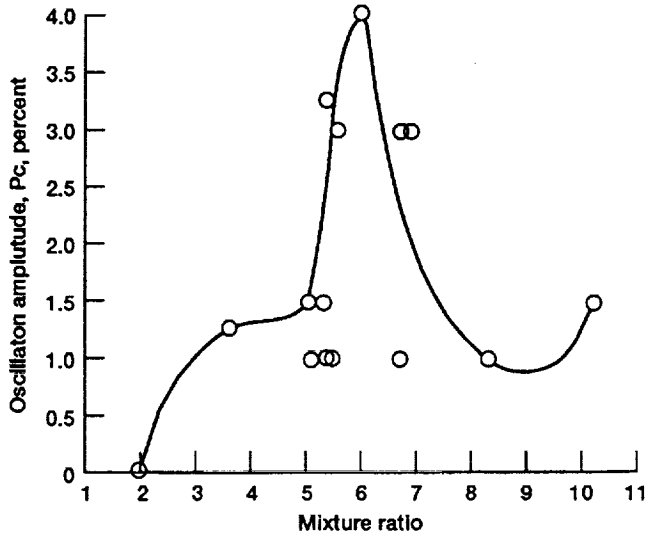

Figure 15.—Variation of oscillation amplitude with mixture ratio (configuration 3, Df - .235").

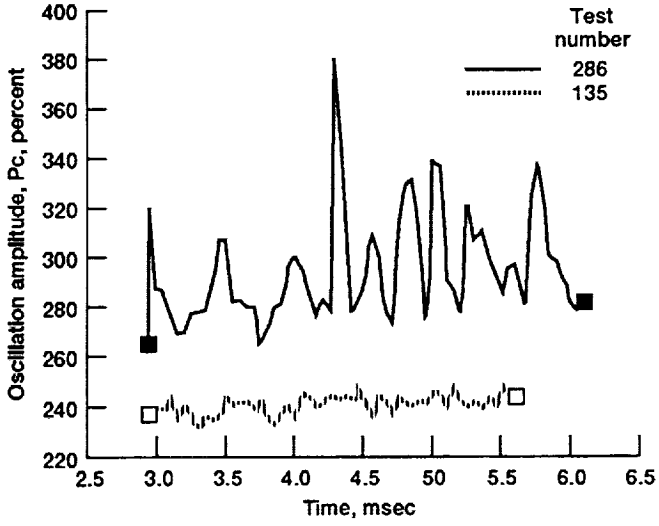

Figure 16.—Computed pressure trace for stable and unstable test cases.

REPORT DOCUMENTATION PAGE

Form Approved
OMB No. 0704-0188

1. AGENCY USE ONLY (*Leave blank*)	2. REPORT DATE	3. REPORT TYPE AND DATES COVERED
	December 1994	Technical Memorandum

4. TITLE AND SUBTITLE

Axisymmetric Single Shear Element Combustion Instability Experiment

5. FUNDING NUMBERS

WU-584-03-11

6. AUTHOR(S)

Kevin J. Breisacher

7. PERFORMING ORGANIZATION NAME(S) AND ADDRESS(ES)

National Aeronautics and Space Administration
Lewis Research Center
Cleveland, Ohio 44135-3191

8. PERFORMING ORGANIZATION REPORT NUMBER

E-8082

9. SPONSORING/MONITORING AGENCY NAME(S) AND ADDRESS(ES)

National Aeronautics and Space Administration
Washington, D.C. 20546-0001

10. SPONSORING/MONITORING AGENCY REPORT NUMBER

NASA TM-106327
AIAA-93-1953
Corrected Copy

11. SUPPLEMENTARY NOTES

Prepared for the 29th Joint Propulsion Conference and Exhibit, cosponsored by the AIAA, SAE, ASME, and ASEE, Monterey, California, June 28-30, 1993. Responsible person, Kevin J. Breisacher, (216) 977-7475.

12a. DISTRIBUTION/AVAILABILITY STATEMENT

Unclassified - Unlimited
Subject Category 20

12b. DISTRIBUTION CODE

13. ABSTRACT (*Maximum 200 words*)

The combustion stability characteristics of a combustor consisting of a single shear element and a cylindrical chamber utilizing LOX and gaseous hydrogen as propellants are presented. The combustor geometry and the resulting longitudinal mode instability are axisymmetric. Hydrogen injection temperature and pyrotechnic pulsing were used to determine stability boundaries. Mixture ratio, fuel annulus gap, and LOX post configuration were varied. Performance and stability data are presented for chamber pressures of 300 and 1000 psia.

14. SUBJECT TERMS

Combustion instability; Rocket engines

15. NUMBER OF PAGES
20

16. PRICE CODE
A03

17. SECURITY CLASSIFICATION OF REPORT	18. SECURITY CLASSIFICATION OF THIS PAGE	19. SECURITY CLASSIFICATION OF ABSTRACT	20. LIMITATION OF ABSTRACT
Unclassified	Unclassified	Unclassified	